

A FRAMEWORK FOR DISCRETE INTEGRAL TRANSFORMATIONS II—THE 2D DISCRETE RADON TRANSFORM*

A. AVERBUCH[†], R. R. COIFMAN[‡], D. L. DONOHO[§], M. ISRAELI[¶], Y. SHKOLNISKY[‡],
AND I. SEDELNIKOV[†]

In memory of Moshe Israeli 1940–2007

Abstract. Although naturally at the heart of many fundamental physical computations, and potentially useful in many important image processing tasks, the Radon transform lacks a coherent discrete definition for two-dimensional (2D) discrete images which is algebraically exact, invertible, and rapidly computable. We define a notion of 2D discrete Radon transforms for 2D discrete images, which is based on summation along lines of absolute slope less than 1. Values at nongrid locations are defined using trigonometric interpolation on a zero-padded grid. Our definition is shown to be geometrically faithful: the summation avoids wrap-around effects. Our proposal uses a special collection of lines in \mathbb{R}^2 for which the transform is rapidly computable and invertible. We describe a fast algorithm using $O(N \log N)$ operations, where $N = n^2$ is the number of pixels in the image. The fast algorithm exploits a discrete projection-slice theorem, which associates the discrete Radon transform with the pseudopolar Fourier transform [A. Averbuch et al., *SIAM J. Sci. Comput.*, 30 (2008), pp. 764–784]. Our definition for discrete images converges to a natural continuous counterpart with increasing refinement.

Key words. Radon transform, projection-slice theorem, linogram, slant stack, pseudopolar Fourier transform, trigonometric interpolation, shearing of digital images

AMS subject classifications. 44A12, 92C55

DOI. 10.1137/060650301

1. Introduction. The Radon transform is a fundamental mathematical tool which appears naturally in many applied settings: medical imaging, radar imaging, nondestructive testing, and geophysical imaging [8].

In dimension 2, the classical Radon transform acts on functions $f(x, y)$ and produces the collection of its line integrals. Let L denote a line inclined at angle θ from the y -axis and at distance t from the origin. The Radon transform $\mathfrak{R}f(\theta, t)$ is defined via

$$\begin{aligned} \mathfrak{R}f(\theta, t) &= \int_L f(x, y) ds \\ (1) \qquad &= \iint_{-\infty}^{\infty} f(x, y) \delta(x \cos \theta + y \sin \theta - t) dx dy, \end{aligned}$$

where $\delta(x)$ is the Dirac delta function.

*Received by the editors January 18, 2006; accepted for publication (in revised form) July 2, 2007; published electronically February 14, 2008.

<http://www.siam.org/journals/sisc/30-2/65030.html>

[†]School of Computer Science, Tel Aviv University, Tel Aviv 69978, Israel (amir@math.tau.ac.il, ilyas@post.tau.ac.il).

[‡]Department of Mathematics, Yale University, New Haven, CT 06520 (coifman@math.yale.edu, yoel.shkolnisky@yale.edu). The fifth author was supported in part by a grant from the Ministry of Science, Israel.

[§]Statistics Department, Stanford University, Stanford, CA 94305 (donoho@stat.stanford.edu).

[¶]Formerly, Faculty of Computer Science, Technion, Haifa 32000, Israel (israeli@cs.technion.ac.il).

There is a fundamental relationship between the two-dimensional (2D) Fourier transform of a function and the one-dimensional (1D) Fourier transform of its Radon transform. This relation is called the “projection-slice theorem,” and for the continuous case it states that the 1D Fourier transform with respect to t of the projection $\mathfrak{R}f(\theta, t)$ is equal to a central slice, at angle θ , of the 2D Fourier transform of the function $f(x, y)$. That is,

$$(2) \quad \widehat{\mathfrak{R}f}(\theta, \xi) = \hat{f}(\xi \cos \theta, \xi \sin \theta),$$

where \hat{f} is the Fourier transform of f [8, 15].

In modern image processing and image representation problems data are discretely sampled images $I = (I(u, v) : u, v = -n/2, \dots, n/2 - 1)$. Despite the discreteness of the data, ideas from the continuous setting can be very helpful and inspiring. Thus, for detecting linear features in images, the Radon transform and cognate tools can suggest useful data processing procedures. Similarly, in developing algorithms for seismic reconstruction, the Radon transform is very suggestive. Unfortunately, there is no really standard notion of a Radon transform for digital data; instead there is a whole forest of proposals—see [3, 4, 5, 16, 17, 14], etc. In this paper we focus on one concrete proposal and argue that it is the most natural one for the setting of discrete images.

1.1. Desiderata. A satisfactory general notion of Radon transform for digital data should have the following properties:

P1. *Algebraic exactness.* The transform should be based on a clear and rigorous definition, not, for example, on analogy; we disapprove of formulations “approximate the integral in (1) by a sum.”

P2. *Geometric fidelity.* The transform should be based on true geometric lines rather than lines which wrap around or are otherwise nongeometric.

P3. *Speed.* The transform should be rapidly computable, for example, admitting an $O(N \log N)$ algorithm, where N is the cardinality of the array I , i.e., $N = n^2$ in the 2D case.

P4. *Invertibility.* The transform should be invertible on its range. Moreover, there should be a fast reconstruction algorithm.

P5. *Parallels with continuum theory.* The transform should obey relations which parallel those of the continuum theory (for example, relations with the Fourier transform).

The many existing contributions to the literature do not offer these properties simultaneously. A complete dissection of the many available notions is beyond hope, so we content ourselves with three examples, which also help to illustrate the meaning of our desiderata above.

- **Fourier approaches.** Some authors [12, 16] have attempted to exploit the projection-slice theorem (2). In the continuum theory, this says that $\mathfrak{R}f(\theta, \cdot)$ can be obtained by (a) performing a 2D Fourier transform, (b) obtaining a radial slice of the Fourier transform, and (c) applying a 1D inverse Fourier transform to the obtained slice. This suggests an algorithm for discrete data, by replacing steps (a) and (c) by fast Fourier transforms (FFTs) for data on 2D and 1D Cartesian grids, respectively. However, strictly speaking, this continuum approach is problematic since step (b) is not naturally defined on digital data: the 2D FFT outputs data in a Cartesian format, while the radial slices of the Fourier domain typically do not intersect the Cartesian grid. Therefore, some sort of interpolation is required, and so the transform

is not algebraically exact. Also, even if the transform should turn out to be invertible (which may be very difficult to determine) the transform is typically not invertible by any straightforward algorithm.

- Multiscale approaches. Other authors [4, 5, 6, 13] have attempted to exploit two-scale relations, which say that if one knows the Radon transform over four dyadic subsquares of a dyadic square, these can be combined to obtain the Radon transform over the larger square. This suggests a recursive algorithm, in which the problem is decomposed into four subproblems, computing Radon transforms over squares of smaller sizes which are then recombined. Strictly speaking, however, the driving identity is a fact about the continuum and does not directly apply to digital arrays, so that when this principle is operationalized, the results involve interpolation and other approximations, and end up being quite crude compared to what we have in mind here. Finally, the use of two-scale relations means that summation along lines is approximated by summation along line segments which are not exactly parallel, and so the results can lack a certain degree of geometric fidelity.
- Algebraic approaches. When n is a prime p , the data grid $G = \{(u, v) : 0 \leq u, v < n\}$ may be considered as the group Z_p^2 , which has very special properties [17]. The “lines” $\{(ka + b \bmod p, kc + d \bmod p) : 0 \leq k < p\}$ for appropriate a, b, c, d have remarkable incidence properties: pairs of lines either do not intersect at all or intersect in just one point. This property makes it possible to define an algebraically exact Radon transform for integration along lines which operates in $O(N \log N)$ flops and is invertible. However, the lines have, for most parameters (a, b, c, d) , very little connection with lines of \mathbb{R}^2 ; simple plots of such lines reveal that they are scattered point sets roughly equidistributed through the grid G . In effect, the lines wrap around (owing to the mod p in their definition), which destroys the geometric fidelity of the transform.

In this paper, we describe a notion of Radon transform for digital data which has all of our desired properties P1–P5. The notion we discuss belongs to a fourth stream of Radon research, complementing the three streams of research just mentioned (Fourier-based methods, multiscale methods, and algebraic approaches) and represents in a certain sense the culmination of that stream. In effect, this fourth stream says that, to really make sense for digital data, the appropriate notions of continuum Radon transform and of discrete 2D Fourier domain are subtly different than the usual ones. Nevertheless, we prove that the discrete Radon transform converges to the continuous Radon transform. This property is of major theoretical and computational importance since it shows that the discrete transform is indeed an approximation of the continuous transform and thus can be used to replace the continuous transform in digital implementations.

Contents. Section 2 defines the 2D discrete Radon transform. The definition in section 2 is derived for discrete images and a continuous set of lines. Section 3 provides a detailed proof of the projection-slice theorem, which associates the discrete Radon transform with the 2D discrete Fourier transform. Section 4 then selects a preferred set of discrete lines underlying a discrete transform, presents the relation between the discrete definition and the pseudopolar Fourier transform [1], and describes fast and accurate forward and inverse algorithms that are based on the pseudopolar Fourier transform. Section 5 proves that the discrete Radon transform converges to the continuous Radon transform as the discretization step goes to zero. Relation to previous

work is discussed in section 6, followed by an interpretation of our construction in section 7. Finally, some concluding remarks are given in section 8.

2. Construction of the transform. We now develop a definition for the Radon transform for discrete data that offers properties P1–P5. Loosely speaking, any discrete Radon transform is defined by summing the samples of $I(u, v)$ along lines. Two key issues: (a) accommodating general lines that do not pass through grid points, (b) choosing a discrete set of lines offering an invertible transform. These issues are dealt with in each of the next two sections.

Our discrete Radon transform sums the discrete samples of the image $I(u, v)$ along lines with absolute slope less than 1. For lines of the form $y = sx + t$ ($|s| \leq 1$), we traverse each line by unit horizontal steps $x = -n/2, \dots, n/2 - 1$; at each x position, we interpolate the image sample at position (x, y) by using trigonometric interpolation in the y -variable. For lines of the form $y = sx + t$ ($|s| \geq 1$), we traverse the line by unit vertical steps in y , interpolating the value at position x using trigonometric interpolation along the corresponding x -variable.

We did not yet restrict the values of s ; s may take any real value in $[-1, 1]$. The requirement for slopes less than 1 induces two families of lines:

basically horizontal line: any line of the form $y = sx + t$, where $|s| \leq 1$.

basically vertical line: any line of the form $x = sy + t$, where $|s| \leq 1$.

Using these line families, we define the 2D Radon transform for discrete images as follows.

DEFINITION 2.1 (2D Radon transform for discrete images). *Let $I(u, v)$, $u, v = -n/2, \dots, n/2 - 1$, be an $n \times n$ array. Let s be a slope such that $|s| \leq 1$, and let t be an intercept such that $t = -n, \dots, n$. Set*

$$(3) \quad \text{Radon}(\{y = sx + t\}, I) = \sum_{u=-n/2}^{n/2-1} \tilde{I}^1(u, su + t),$$

$$(4) \quad \text{Radon}(\{x = sy + t\}, I) = \sum_{v=-n/2}^{n/2-1} \tilde{I}^2(sv + t, v),$$

where

$$(5) \quad \tilde{I}^1(u, y) = \sum_{v=-n/2}^{n/2-1} I(u, v) D_m(y - v), \quad u = -n/2, \dots, n/2 - 1, \quad y \in \mathbb{R},$$

$$(6) \quad \tilde{I}^2(x, v) = \sum_{u=-n/2}^{n/2-1} I(u, v) D_m(x - u), \quad v = -n/2, \dots, n/2 - 1, \quad x \in \mathbb{R},$$

and D_m is the Dirichlet kernel

$$(7) \quad D_m(t) = \frac{\sin(\pi t)}{m \sin(\pi t/m)}, \quad m = 2n + 1.$$

For an arbitrary line l with slope s and intercept t , such that $|s| \leq 1$ and $t = -n, \dots, n$, the Radon transform is given by

$$(8) \quad (RI)(s, t) = \begin{cases} \text{Radon}(\{y = sx + t\}, I), & l \text{ is a basically horizontal line,} \\ \text{Radon}(\{x = sy + t\}, I), & l \text{ is a basically vertical line.} \end{cases}$$

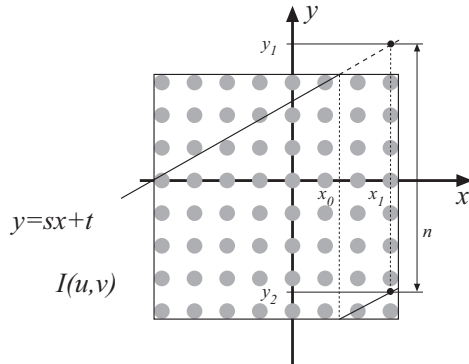


FIG. 1. Summation of wrap-around line without padding.

\tilde{I}^1 and \tilde{I}^2 in (5) and (6) are columnwise and rowwise interpolated versions of I , respectively, using the Dirichlet kernel D_m with $m = 2n + 1$.

2.1. Selection of the parameters t and m . Our condition $|s| \leq 1$ implicitly partitions the collection of oriented lines in the plane into the basically vertical and the basically horizontal lines and, moreover, gives a complete symmetry in handling basically horizontal and vertical lines. Each result for basically horizontal lines will apply analogously to basically vertical lines, and vice versa.

Hence, once s is fixed, it remains to find the range t of relevant intercepts. Section 4 will show that using $t = -n, \dots, n$ ensures that the transform is invertible, and moreover, when considering the analogy to the continuous case, this range of t provides us with all the lines that intersect the bounding box of $I(u, v)$ (nontrivial projections).

Next, we explain the requirement $m = 2n + 1$. One’s initial impulse would no doubt be to use $m = n$, which is standard in trigonometric interpolation. This would give us D_n instead of D_m . Taking some line $y = sx + t$ (Figure 1) with value y_1 at x_1 , we would obtain from (5)

$$\tilde{I}^1(x_1, y_1) = \sum_{v=-n/2}^{n/2-1} I(x_1, v)D_n(y_1 - v).$$

It is easy to verify that if $y_2 = y_1 - n$, then (see Figure 1)

$$(9) \quad \tilde{I}^1(x_1, y_1) = \pm \sum_{v=-n/2}^{n/2-1} I(x_1, v)D_n(y_2 - v).$$

Equation (9) states that evaluating \tilde{I}^1 at a point y_1 would be the same (in absolute value) as evaluating \tilde{I}^1 at the point $y_1 - n$. Concretely, evaluating \tilde{I}^1 at $y_1 = n/2$, which is outside the domain of $I(u, v)$ and therefore should be interpolated as a small value, would be the same as evaluating \tilde{I}^1 at $y = -n/2$, which is a true sample of $I(u, v)$. In short, our “lines” actually would wrap around as in Figure 1, and would not be true geometric lines.

To eliminate the wrap-around effect, we pad I with zeros (see Figure 2); although the periodic nature of the Dirichlet kernel persists, the periodization interacts

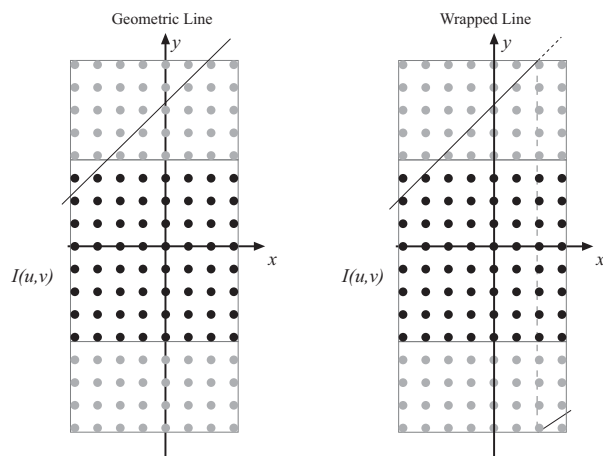


FIG. 2. Summation of wrap-around line with padding.

with zeros outside the image and has no effect. Figure 2 gives an illustration of geometric and wrapped lines in a padded image. Although the line on the right image exhibits wraparound, the wraparound is over zeros and not over true samples of $I(u, v)$. According to our choice of s and t , it follows that a line $y = sx + t$ with $x = -n/2, \dots, n/2 - 1$ satisfies $y < 3n/2$ at $x = n/2 - 1$. When wraparound is taken into consideration (due to periodicity of length $m = 2n + 1$), this y is identical to $y_1 = y - (2n + 1) < -n/2$. Hence, we pad I symmetrically with at least $n + 1$ zeros to separate y_1 (the wrapped-around version of y) from true samples of I . We conclude that setting $m = 2n + 1$ ensures that samples with $n/2 \leq y < 3n/2$ do not overlap with samples of I having $-n/2 \leq y < n/2$.

When basically vertical lines are considered, symmetry leads to the same result; i.e., we have to use an interpolation kernel D_m with $m = 2n + 1$.

2.2. Representation of lines using angles. In order to derive the 2D Radon transform (Definition 2.1) in a more natural way, we parametrize lines using angles instead of slopes. For a basically horizontal line $y = sx + t$ with $|s| \leq 1$, write $s = \tan \theta$ with $\theta \in [-\pi/4, \pi/4]$, the angle between the line and the positive x -axis. Using this notation, a basically horizontal line has the form $y = (\tan \theta)x + t$ with $\theta \in [-\pi/4, \pi/4]$. Given a basically vertical line $x = sy + t$ with $|s| \leq 1$, write $s = \cot \theta$ with $\theta \in [\pi/4, 3\pi/4]$, where θ is again the angle between the line and the positive x -axis. Hence, a basically vertical line has the form $x = (\cot \theta)y + t$ with $\theta \in [\pi/4, 3\pi/4]$.

Using this parametric representation, we rephrase our definition of Radon transform (Definition 2.1) as follows.

DEFINITION 2.2. Let $I(u, v)$, $u, v = -n/2, \dots, n/2 - 1$, be an $n \times n$ array. Let $\theta \in [-\pi/4, 3\pi/4]$ and $t = -n, \dots, n$. Set

$$(10) \quad R_\theta I(t) = \begin{cases} \text{Radon}(\{y = (\tan \theta)x + t\}, I), & \theta \in [-\pi/4, \pi/4], \\ \text{Radon}(\{x = (\cot \theta)y + t\}, I), & \theta \in [\pi/4, 3\pi/4], \end{cases}$$

where $\text{Radon}(\{y = sx + t\}, I)$ and $\text{Radon}(\{x = sy + t\}, I)$ are given in (3) and (4), respectively.

The Radon transform in Definition 2.2 operates on discrete images $I(u, v)$ while θ is continuous. In section 4 we discretize the parameter θ in order to get a “discrete Radon transform” that satisfies properties P1–P5 given in section 1.

3. Projection-slice theorem. The continuous projection-slice theorem (2) allows us to evaluate the continuous Radon transform using the 2D Fourier transform. A similar relation exists connecting our discrete Radon transform and the discrete Fourier transform of an image. We later exploit it to develop an algorithm.

To construct such a relation we define some auxiliary operators which enable us to rephrase the definition of the discrete Radon transform (Definition 2.2) in a more convenient way. Throughout this section we denote by \mathbb{C}^m the set of complex-valued vectors of length m , indexed from $-\lfloor m/2 \rfloor$ to $\lfloor (m-1)/2 \rfloor$. Also, we denote by $\mathbb{C}^{k \times l}$ the set of 2D complex-valued arrays of dimensions $k \times l$. Each array $I \in \mathbb{C}^{k \times l}$ is structured as $I(u, v)$, where $u = -\lfloor k/2 \rfloor, \dots, \lfloor (k-1)/2 \rfloor$ and $v = -\lfloor l/2 \rfloor, \dots, \lfloor (l-1)/2 \rfloor$.

DEFINITION 3.1 (translation operator). Let $m = 2n + 1$. Let $\alpha \in \mathbb{C}^m$ and $\tau \in \mathbb{R}$. The translation operator $T_\tau : \mathbb{C}^m \rightarrow \mathbb{C}^m$ is given by

$$(11) \quad (T_\tau \alpha)_u = \sum_{i=-n}^n \alpha_i D_m(u - i - \tau),$$

where $u = -n, \dots, n$ and D_m is given by (7).

The translation operator T_τ takes a vector of length m and translates it by τ by using trigonometric interpolation.

LEMMA 3.2. Let T_τ be the translation operator given by Definition 3.1. Then,

$$\text{adj } T_\tau = T_{-\tau}.$$

The proof easily follows from Definition 3.1 and the fact that $D_m(t)$ is an even function.

An important property of the translation operator T_τ is that the translation of exponentials is algebraically exact. In other words, translating a vector of samples of the exponential $e^{2\pi i k x/m}$ is the same as resampling the exponential at the translated points. This observation is of great importance for proving the projection-slice theorem.

LEMMA 3.3. Let $m = 2n + 1$, $\varphi(x) = e^{2\pi i k x/m}$. Define the vector $\phi \in \mathbb{C}^m$ as $\phi = (\varphi(t) : t = -n, \dots, n)$. Then, for arbitrary $\tau \in \mathbb{R}$,

$$(T_\tau \phi)_t = \varphi(t - \tau), \quad t = -n, \dots, n.$$

Proof. $x \mapsto (T_\tau \phi)_x$ and $\varphi(x - \tau)$, $x \in \mathbb{R}$, are two trigonometric polynomials of degree n that coincide on $m = 2n + 1$ points $t = -n, \dots, n$ [19]. \square

DEFINITION 3.4. The extension operators $E^1 : \mathbb{C}^{n \times n} \rightarrow \mathbb{C}^{n \times m}$ and $E^2 : \mathbb{C}^{n \times n} \rightarrow \mathbb{C}^{m \times n}$ are given by

$$(12) \quad E^i I(u, v) = \begin{cases} I(u, v), & u, v = -n/2, \dots, n/2 - 1, \\ 0, & \text{otherwise,} \end{cases}$$

for $i = 1, 2$, where $m = 2n + 1$.

E^1 zero pads an $n \times n$ image to size $(2n + 1) \times n$ ($2n + 1$ rows and n columns) by adding $n/2 + 1$ zero rows at the top of the array and $n/2$ zero rows at the bottom of the array. Similarly, E^2 corresponds to padding the array I with $n + 1$ zero columns, $n/2 + 1$ at the right and $n/2$ at the left.

DEFINITION 3.5. The truncation operators $U^1 : \mathbb{C}^{n \times m} \rightarrow \mathbb{C}^{n \times n}$ and $U^2 : \mathbb{C}^{m \times n} \rightarrow \mathbb{C}^{n \times n}$ are given by

$$(13) \quad U^i I(u, v) = I(u, v), \quad u, v = -n/2, \dots, n/2 - 1,$$

where $i = 1, 2$ and $m = 2n + 1$.

The operator U^1 removes $n/2 + 1$ rows from the top of the array and $n/2$ rows from the bottom of the array, recovering an $n \times n$ image. Similarly, U^2 removes $n/2 + 1$ columns from the right and $n/2$ columns from the left of the array.

LEMMA 3.6. *Let E^i and U^i , $i = 1, 2$, be the extension and truncation operators, given by Definitions 3.4 and 3.5, respectively. Then,*

$$\text{adj } E^1 = U^1, \quad \text{adj } E^2 = U^2.$$

DEFINITION 3.7. *Let $I(u, v)$, $u, v = -n/2, \dots, n/2 - 1$, be an $n \times n$ image. The shearing operators $S^1 : \mathbb{C}^{n \times m} \rightarrow \mathbb{C}^{n \times m}$ and $S^2 : \mathbb{C}^{m \times n} \rightarrow \mathbb{C}^{m \times n}$, $m = 2n + 1$, are given by*

$$(14) \quad (S^1_\theta I)(u, v) = (T_{-u \tan \theta} I(u, \cdot))_v, \quad \theta \in [-\pi/4, \pi/4],$$

$$(15) \quad (S^2_\theta I)(u, v) = (T_{-v \cot \theta} I(\cdot, v))_u, \quad \theta \in [\pi/4, 3\pi/4].$$

Combining Definitions 2.2, 3.7, and 3.1 we obtain the following lemma.

LEMMA 3.8. *For $t = -n, \dots, n$,*

$$R_\theta I(t) = \begin{cases} \sum_{u=-n/2}^{n/2-1} (S^1_\theta(E^1 I))(u, t), & \theta \in [-\pi/4, \pi/4], \\ \sum_{v=-n/2}^{n/2-1} (S^2_\theta(E^2 I))(t, v), & \theta \in [\pi/4, 3\pi/4]. \end{cases}$$

DEFINITION 3.9. *Let $\psi \in \mathbb{C}^m$, $m = 2n + 1$. The backprojection operators $B^1_\theta : \mathbb{C}^m \rightarrow \mathbb{C}^{n \times m}$ and $B^2_\theta : \mathbb{C}^m \rightarrow \mathbb{C}^{m \times n}$ are given by*

$$(16) \quad \begin{aligned} (B^1_\theta \psi)(u, \cdot) &= T_{u \tan \theta} \psi, & \theta \in [-\pi/4, \pi/4], \\ (B^2_\theta \psi)(\cdot, v) &= T_{v \cot \theta} \psi, & \theta \in [\pi/4, 3\pi/4]. \end{aligned}$$

LEMMA 3.10.

$$(17) \quad \text{adj } B^1_\theta = \sum_u S^1_\theta,$$

$$(18) \quad \text{adj } B^2_\theta = \sum_v S^2_\theta.$$

The proof easily follows from Definitions 3.7 and 3.9 and from Lemma 3.2.

From Lemmas 3.8, 3.6, and 3.10 we get the following formula for the adjoint Radon transform.

THEOREM 3.11. *The adjoint Radon transform $\text{adj } R_\theta : \mathbb{C}^m \rightarrow \mathbb{C}^{n \times n}$ is given by*

$$(19) \quad \text{adj } R_\theta = \begin{cases} U^1 \circ B^1_\theta, & \theta \in [-\pi/4, \pi/4], \\ U^2 \circ B^2_\theta, & \theta \in [\pi/4, 3\pi/4], \end{cases}$$

where U^i , $i = 1, 2$, is given by Definition 3.5 and B^i_θ , $i = 1, 2$, is given by Definition 3.9.

We next examine how the adjoint Radon transform operates on the vector $\phi^{(k)} = (\varphi^{(k)}(t) : t = -n, \dots, n)$, where $\varphi^{(k)}(t) = e^{2\pi ikt/m}$. For $\theta \in [-\pi/4, \pi/4]$ and $u, v =$

$-n/2, \dots, n/2 - 1$ we have

$$\begin{aligned} (\text{adj } R_\theta \phi^{(k)})(u, v) &= (U^1 B_\theta^1 \phi^{(k)})(u, v) && \text{(by Theorem 3.11)} \\ &= (B_\theta^1 \phi^{(k)})(u, v) = (T_{u \tan \theta} \phi^{(k)})_v && \text{(by (16))} \\ &= \varphi^{(k)}(v - u \tan \theta) && \text{(by Lemma 3.3)} \\ &= e^{\frac{2\pi i}{m} k(v - u \tan \theta)}. \end{aligned}$$

Similarly, for $\theta \in [\pi/4, 3\pi/4]$ and $u, v = -n/2, \dots, n/2 - 1$ we get

$$(20) \quad (\text{adj } R_\theta \phi^{(k)})(u, v) = e^{\frac{2\pi i}{m} k(u - v \cot \theta)}.$$

THEOREM 3.12 (projection-slice theorem). *Let $I(u, v)$ be an $n \times n$ image, $u, v = -n/2, \dots, n/2 - 1$, and let $m = 2n + 1$. Then,*

$$(\widehat{R_\theta I})(k) = \begin{cases} \hat{I}(-s_1 k, k), & s_1 = \tan \theta, & \theta \in [-\pi/4, \pi/4], \\ \hat{I}(k, -s_2 k), & s_2 = \cot \theta, & \theta \in [\pi/4, 3\pi/4], \end{cases}$$

where $\widehat{R_\theta I}(k)$ denotes the 1D discrete Fourier transform (DFT) of the discrete Radon transform (Definition 2.2), with respect to the index t , $k = -n, \dots, n$, and \hat{I} is the trigonometric polynomial

$$(21) \quad \hat{I}(\xi_1, \xi_2) = \sum_{u=-n/2}^{n/2-1} \sum_{v=-n/2}^{n/2-1} I(u, v) e^{-\frac{2\pi i}{m} (\xi_1 u + \xi_2 v)}.$$

Proof. Define $\phi_j^{(k)} = e^{\frac{2\pi i}{m} k j}$. For $\theta \in [-\pi/4, \pi/4]$ we have

$$\begin{aligned} \widehat{R_\theta I}(k) &= \sum_{j=-n}^n R_\theta I(j) e^{-2\pi i k j / m} \\ &= \langle R_\theta I, \phi^{(k)} \rangle \\ &= \langle I, (\text{adj } R_\theta) \phi^{(k)} \rangle \\ &= \sum_{u=-n/2}^{n/2-1} \sum_{v=-n/2}^{n/2-1} I(u, v) e^{-\frac{2\pi i}{m} k(v - s_1 u)} \\ &= \hat{I}(-s_1 k, k), \end{aligned}$$

where \hat{I} is the trigonometric polynomial given by (21).

The proof for $\theta \in [\pi/4, 3\pi/4]$ is similar. \square

4. Discretization and fast algorithms. The Radon transform, given by Definition 2.2, and the projection-slice theorem, given by Theorem 3.12, were defined for discrete images and any arbitrary line. Specifically, $R_\theta I(t)$ is defined for any angle in the range $[-\pi/4, 3\pi/4]$. For a digital implementation, we must discretize the set of lines. We index these by angles Θ defined as follows:

$$(22) \quad \Theta \triangleq \Theta_1 \cup \Theta_2,$$

where

$$(23) \quad \Theta_2 = \{ \arctan(2l/n) \mid l = -n/2, \dots, n/2 \},$$

$$(24) \quad \Theta_1 = \{ \pi/2 - \arctan(2l/n) \mid l = -n/2, \dots, n/2 \}.$$

In words, Θ_1 indexes the basically vertical lines and Θ_2 indexes the basically horizontal lines. Note that for two elements $\theta_2^l, \theta_2^{l+1} \in \Theta_2$, $\tan \theta_2^{l+1} - \tan \theta_2^l = \frac{2}{n}$, which means that our angles define a set of lines with equally spaced slopes. By using the discrete set of intercepts

$$(25) \quad T \triangleq \{-n, \dots, n\},$$

we are able to state the following.

DEFINITION 4.1. *The digital Radon transform for an $n \times n$ image I is a $2n + 2$ times $2n + 1$ array*

$$(26) \quad RI = \{ R_\theta I(t) \mid \theta \in \Theta, t \in T \}.$$

Theorem 3.12 holds for arbitrary angles, and in particular for the discrete set Θ . For $\theta \in \Theta^2$ (see (23)) we have from Theorem 3.12 that $\widehat{R_\theta I}(k) = \hat{I}(-s_1 k, k)$, where $s_1 = \tan \theta$. Since $\theta \in \Theta^2$ has the form $\theta = \arctan(2l/n)$, it follows that $s_1 = 2l/n$ and

$$(27) \quad \widehat{R_\theta I}(k) = \hat{I}\left(-\frac{2l}{n}k, k\right), \quad k = -n, \dots, n.$$

For $\theta \in \Theta^1$ (see (24)), we have from Theorem 3.12 that $\widehat{R_\theta I}(k) = \hat{I}(k, -s_2 k)$, where $s_2 = \cot \theta$. Since $\theta \in \Theta^1$ has the form $\theta = \pi/2 - \arctan(2l/n)$, it follows that $s_2 = 2l/n$ and

$$(28) \quad \widehat{R_\theta I}(k) = \hat{I}\left(k, -\frac{2l}{n}k\right), \quad k = -n, \dots, n.$$

Equations (27) and (28) show that $\widehat{R_\theta I}$ is obtained by evaluating the trigonometric polynomial \hat{I} , given by (21), at nodes of the grid Ω_{pp} , defined in [1] as

$$(29) \quad \Omega_{pp} \triangleq \Omega_{pp}^1 \cup \Omega_{pp}^2,$$

where

$$(30) \quad \Omega_{pp}^1 \triangleq \left\{ \left(-\frac{2l}{n}k, k \right) \mid -n/2 \leq l \leq n/2, -n \leq k \leq n \right\},$$

$$(31) \quad \Omega_{pp}^2 \triangleq \left\{ \left(k, -\frac{2l}{n}k \right) \mid -n/2 \leq l \leq n/2, -n \leq k \leq n \right\}.$$

Specifically, if we use the notation $\hat{I}_{\Omega_{pp}^1}$ and $\hat{I}_{\Omega_{pp}^2}$ to denote the samples of \hat{I} (see (21)) on the sets Ω_{pp}^1 and Ω_{pp}^2 , respectively, then,

$$(32) \quad \widehat{R_\theta I}(k) = \hat{I}_{\Omega_{pp}^1}(k, l), \quad \theta \in \Theta^2,$$

$$(33) \quad \widehat{R_\theta I}(k) = \hat{I}_{\Omega_{pp}^2}(k, l), \quad \theta \in \Theta^1,$$

or equivalently,

$$(34) \quad \begin{aligned} R_\theta I &= F_k^{-1} \circ \hat{I}_{\Omega_{pp}^1}, & \theta \in \Theta^2, \\ R_\theta I &= F_k^{-1} \circ \hat{I}_{\Omega_{pp}^2}, & \theta \in \Theta^1, \end{aligned}$$

where F_k^{-1} is the 1D inverse Fourier transform along each row of the array $\hat{I}_{\Omega_{pp}^j}$, $j = 1, 2$ (along the index k).

The fast algorithm that computes the pseudopolar Fourier transform [1] immediately gives an algorithm for computing the discrete Radon transform. To see this, consider a row in RI (see (26)), which corresponds to a constant θ . The values of the discrete Radon transform that correspond to θ are computed by applying F_k^{-1} to a row of $\hat{I}_{\Omega_{pp}^j}$, $j = 1, 2$. Thus, the computation of RI requires application of F_k^{-1} to all rows of $\hat{I}_{\Omega_{pp}^j}$, $j = 1, 2$ ($2n + 2$ rows). Since each application of F_k^{-1} requires $O(n \log n)$ operations, we get a total of $O(n^2 \log n)$ operations for the required $2n + 2$ calls to F_k^{-1} . Thus, once we compute the arrays $\hat{I}_{\Omega_{pp}^j}$, $j = 1, 2$, it requires $O(n^2 \log n)$ operations to compute RI . Since computing $\hat{I}_{\Omega_{pp}^j}$, $j = 1, 2$, requires $O(n^2 \log n)$ operations [1], the total complexity of computing the values of RI is $O(n^2 \log n)$ operations.

Invertibility of the 2D discrete Radon transform RI also follows from (34). F_k^{-1} is invertible and can be rapidly inverted by using the FFT. $\hat{I}_{\Omega_{pp}^j}$ is invertible and can be rapidly inverted as described in [1]. Thus, the discrete Radon transform is invertible and can be inverted by applying the FFT on each row of RI ($O(n^2 \log n)$ operations), followed by an inversion of $\hat{I}_{\Omega_{pp}^j}$ ($O(n^2 \log n)$ operations). Hence, inverting the discrete Radon transform requires $O(n^2 \log n)$ operations.

5. Convergence. In this section we prove that the discrete Radon transform converges to the continuous Radon transform as the discretization step goes to zero.

5.1. Alternative representation of the continuous Radon transform. In this section we use a definition of the continuous Radon transform which is equivalent to (1) but that is more convenient for subsequent derivations. We divide the set of all lines in \mathbb{R}^2 into basically horizontal and basically vertical lines (section 2). We denote the Radon transform of f along basically horizontal lines by $\mathfrak{R}_x f$ and along basically vertical lines by $\mathfrak{R}_y f$. For a basically horizontal line $y = sx + t$, $s \in [-1, 1]$, the integral of f along this line is given by

$$(35) \quad \mathfrak{R}_x f(s, t) = \sqrt{1 + s^2} \int_{-\infty}^{\infty} f(x, t + sx) dx.$$

For a basically vertical line $x = sy + t$, $s \in [-1, 1]$, the integral of f along this line is given by

$$(36) \quad \mathfrak{R}_y f(s, t) = \sqrt{1 + s^2} \int_{-\infty}^{\infty} f(t + sy, y) dy.$$

When the function $f(x, y)$ has a finite support, the limits of integration in (35) and (36) become finite. Indeed, assume that there exists a positive constant D such that $f(x, y) = 0$ whenever $|x| \geq \frac{D}{2}$ or $|y| \geq \frac{D}{2}$. This ensures that all vertical and horizontal shears of $f(x, y)$ fit into a square of size $D \times D$. Then, for any $s \in [-1, 1]$ we have

$$(37) \quad \mathfrak{R}_x f(s, t) = \sqrt{1 + s^2} \int_{-D}^D f(x, t + sx) dx$$

for $t \in [-D, D]$ and $\Re_x f(s, t) = 0$ otherwise. Similarly,

$$(38) \quad \Re_y f(s, t) = \sqrt{1 + s^2} \int_{-D}^D f(t + sy, y) dy$$

for $t \in [-D, D]$ and $\Re_y f(s, t) = 0$ otherwise.

5.2. Mathematical preliminaries. A 1D trigonometric polynomial of order N is an expression of the form

$$T(x) = \sum_{n=-N}^N c_n e^{inx},$$

where c_n are complex numbers. Similarly, a 2D trigonometric polynomial of order N is an expression of the form

$$T(x, y) = \sum_{k=-N}^N \sum_{l=-N}^N c_{k,l} e^{i(kx+ly)},$$

where $c_{k,l}$ are complex numbers.

THEOREM 5.1 (uniqueness of a trigonometric interpolating polynomial; see [19]). *Given $2N + 1$ points $x_{-N}, \dots, x_0, \dots, x_N$, which are distinct modulo 2π , and arbitrary numbers $y_{-N}, \dots, y_0, \dots, y_N$, there always exists a unique trigonometric polynomial such that $T(x_k) = y_k, k = -N, \dots, N$.*

The polynomial $T(x)$ is called the (trigonometric) interpolating polynomial that corresponds to points x_k and values y_k . Given a function $f : \mathbb{R} \rightarrow \mathbb{R}$, the 1D trigonometric interpolating polynomial of degree N corresponding to points $\{\frac{2\pi}{M}u\}_{u=-N}^N$ and values $\{f(\frac{2\pi}{M}u)\}_{u=-N}^N$ is given explicitly by

$$(39) \quad f_N(x) = \sum_{n=-N}^N f\left(\frac{2\pi}{M}n\right) D_M\left(n - \frac{M}{2\pi}x\right),$$

where $D_M(x)$ is the Dirichlet kernel given by (7). Similarly, for a function $f : \mathbb{R}^2 \rightarrow \mathbb{R}$, the 2D trigonometric interpolating polynomial of degree N corresponding to points $\{(\frac{2\pi}{M}u, \frac{2\pi}{M}v)\}_{u,v=-N}^N$ and values $\{f(\frac{2\pi}{M}u, \frac{2\pi}{M}v)\}_{u,v=-N}^N$ is explicitly given by

$$f_N(x, y) = \sum_{u=-N}^N \sum_{v=-N}^N f\left(\frac{2\pi}{M}u, \frac{2\pi}{M}v\right) D_M\left(u - \frac{M}{2\pi}x\right) D_M\left(v - \frac{M}{2\pi}y\right).$$

DEFINITION 5.2. Let $D \in \mathbb{R}^+, f : \mathbb{R}^2 \rightarrow \mathbb{R}$. We define

$$f_N^D(x, y) \triangleq \sum_{u=-N}^N \sum_{v=-N}^N f\left(\frac{2D}{M}u, \frac{2D}{M}v\right) D_M\left(u - \frac{M}{2D}x\right) D_M\left(v - \frac{M}{2D}y\right).$$

Note that when $D = \pi$, we have $f_N^D(x, y) = f_N(x, y)$.

LEMMA 5.3. Let $f : \mathbb{R}^2 \rightarrow \mathbb{R}, N \in \mathbb{N}, v \in [-N : N]$. Then, for $g(x) \triangleq f(x, \frac{2\pi}{M}v)$ we have $g_N(x) = f_N(x, \frac{2\pi}{M}v)$.

Proof. The function $f_N(x, \frac{2\pi}{M}v)$ is a trigonometric polynomial of degree N in x . For any $u \in [-N : N]$ we have $f_N(\frac{2\pi}{M}u, \frac{2\pi}{M}v) = f(\frac{2\pi}{M}u, \frac{2\pi}{M}v) = g(\frac{2\pi}{M}u)$. The lemma now follows from Theorem 5.1 (uniqueness of the 1D trigonometric interpolating polynomial). \square

DEFINITION 5.4 (Lipschitz class $Lip_C(\alpha, \Omega)$). Let $\Omega \subseteq \mathbb{R}^n$. If $f : \mathbb{R}^n \rightarrow \mathbb{R}$ satisfies the condition

$$|f(x) - f(y)| \leq C\|x - y\|^\alpha, \quad 0 < \alpha \leq 1,$$

for all $x, y \in \Omega$, then we say that f belongs to the class $Lip_C(\alpha, \Omega)$. When the value of the constant C is not important, we say that f is Lipschitz α on Ω .

LEMMA 5.5 (uniform convergence of a shifted interpolation; see [18]). Let $A \in [0, \pi]$, $C \in \mathbb{R}^+$, $\alpha \in (0, 1]$, $N \in \mathbb{N}$. Let $f(x) \in Lip_C(\alpha, \mathbb{R})$ such that $f(x) = 0$ whenever $|x| \geq A$. Then, for any $|\delta| \leq \pi - A$ we have

$$|f_N(x - \delta) - f(x - \delta)| \leq \Phi(C, \alpha, N), \quad x \in [-\pi, \pi],$$

where $f_N(x)$ is given by (39) and $\Phi(C, \alpha, N)$ is a function independent of both f and A such that $\lim_{N \rightarrow \infty} \Phi(C, \alpha, N) = 0$.

DEFINITION 5.6. Let $s \in [-1, 1]$, $f : \mathbb{R}^2 \rightarrow \mathbb{R}$. The horizontal shear of f , denoted $f_s(x, y)$, is defined as $f_s(x, y) \triangleq f(x + sy, y)$.

LEMMA 5.7. Let $f \in Lip_C(\alpha, \mathbb{R}^2)$. Then, for any $s \in [-1, 1]$ we have $f_s \in Lip_{(\sqrt{3})^\alpha C}(\alpha, \mathbb{R}^2)$.

Proof. Since $f(x, y)$ is Lipschitz, for any two points in \mathbb{R}^2 we have

$$\begin{aligned} |f_s(x_1, y_1) - f_s(x_2, y_2)| &= |f(x_1 + sy_1, y_1) - f(x_2 + sy_2, y_2)| \\ &\leq C \left(\sqrt{((x_1 - x_2) + s(y_1 - y_2))^2 + (y_1 - y_2)^2} \right)^\alpha. \end{aligned}$$

For $s \in [-1, 1]$ and for any $x, y \in \mathbb{R}^2$ we have

$$(x + sy)^2 + y^2 \leq x^2 + 2|x||y| + y^2 + y^2 \leq 3(x^2 + y^2).$$

Therefore,

$$|f_s(x_1, y_1) - f_s(x_2, y_2)| \leq (\sqrt{3})^\alpha C \left(\sqrt{(x_1 - x_2)^2 + (y_1 - y_2)^2} \right)^\alpha. \quad \square$$

The following lemma easily follows by using the mean value theorem for integrals.

LEMMA 5.8. Let $C \in \mathbb{R}^+$, $\alpha \in (0, 1]$, $t_1, t_2 \in \mathbb{R}$ such that $t_1 < t_2$. Consider $f \in Lip_C(\alpha, [t_1, t_2])$ and $\xi \in [t_1, t_2]$. Then,

$$\left| \int_{t_1}^{t_2} f(x) dx - f(\xi)(t_2 - t_1) \right| \leq C|t_2 - t_1|^{1+\alpha}.$$

5.3. Discretization of the continuous Radon transform. We next consider the discretization of the integral from (38). First, we consider this integral for $s = 0$.

DEFINITION 5.9. Let $D \in \mathbb{R}^+$, $f \in C^0(\mathbb{R}^2)$. For an arbitrary $x \in \mathbb{R}$ we define

$$T[D, f](x) \triangleq \int_{-D}^D f(x, y) dy.$$

DEFINITION 5.10. Let $N \in \mathbb{N}$, $M = 2N + 1$. Let $D \in \mathbb{R}^+$, $f : \mathbb{R}^2 \rightarrow \mathbb{R}$. For an arbitrary $x \in \mathbb{R}$ we define

$$T_N[D, f](x) \triangleq \frac{2D}{M} \sum_{v=-N}^N f\left(x, \frac{2D}{M}v\right).$$

THEOREM 5.11 (approximation of the vertical Radon transform). Let $D \in \mathbb{R}^+$, $C \in \mathbb{R}^+$, $\alpha \in (0, 1]$. Let $N \in \mathbb{N}$, $M = 2N + 1$. Denote $\Omega = \{(x, y) \mid x, y \in [-D, D]\}$. Then, $T_N[D, f](x)$ converges to $T[D, f](x)$ uniformly in both $f \in Lip_C(\alpha, \Omega)$ and $x \in [-D, D]$.

Proof. Let us fix $f \in Lip_C(\alpha, \Omega)$ and $x \in [-D, D]$. We define $f_x(y) \triangleq f(x, y)$. Then,

$$|T[D, f](x) - T_N[D, f](x)| = \left| \int_{-D}^D f_x(y) dy - \frac{2D}{M} \sum_{v=-N}^N f_x\left(\frac{2D}{M}v\right) \right|.$$

For $v \in [-N : N]$ we define $\xi_v \triangleq \frac{2D}{M}v$. The interval $[-D, D]$ is a union of the subintervals $[\xi_v - \frac{D}{M}, \xi_v + \frac{D}{M}]$, $v \in [-N : N]$. Then,

$$(40) \quad |T[D, f](x) - T_N[D, f](x)| = \left| \sum_{v=-N}^N \int_{\xi_v - \frac{D}{M}}^{\xi_v + \frac{D}{M}} f_x(y) dy - \sum_{v=-N}^N \frac{2D}{M} f_x(\xi_v) \right|.$$

Since f belongs to $Lip_C(\alpha, \Omega)$, we have $f_x \in Lip_C(\alpha, [-D, D])$. From Lemma 5.8 we have for an arbitrary $v \in [-N : N]$

$$(41) \quad \left| \int_{\xi_v - \frac{D}{M}}^{\xi_v + \frac{D}{M}} f_x(y) dy - \frac{2D}{M} f_x(\xi_v) \right| \leq C \left(\frac{2D}{M} \right)^{1+\alpha}.$$

Applying the triangle inequality to (40) and using (41), we get

$$\begin{aligned} |T[D, f](x) - T_N[D, f](x)| &\leq \sum_{v=-N}^N \left| \int_{\xi_v - \frac{D}{M}}^{\xi_v + \frac{D}{M}} f_x(y) dy - \frac{2D}{M} f_x(\xi_v) \right| \\ &\leq MC \left(\frac{2D}{M} \right)^{1+\alpha} = 2DC \left(\frac{2D}{M} \right)^{\alpha}. \end{aligned}$$

The last expression tends to zero as N grows, and it depends neither on x nor on f . \square

DEFINITION 5.12. Let $s \in [-1, 1]$. Let $D \in \mathbb{R}^+$, $f \in C^0(\mathbb{R}^2)$. For an arbitrary x we define

$$T^s[D, f](x) \triangleq \int_{-D}^D f(x + sy, y) dy.$$

Note that $T^s[D, f](x) = T[D, f_s](x)$.

DEFINITION 5.13. Let $s \in [-1, 1]$, $N \in \mathbb{N}$, $M = 2N + 1$. Let $f : \mathbb{R}^2 \rightarrow \mathbb{R}$. For an arbitrary $x \in \mathbb{R}$ we define

$$(42) \quad T_N^s[D, f](x) \triangleq \frac{2D}{M} \sum_{v=-N}^N f\left(x + s \frac{2D}{M}v, \frac{2D}{M}v\right).$$

Note that $T_N^s[D, f](x) = T_N[D, f_s](x)$.

THEOREM 5.14 (approximation of the vertical Radon transform of a sheared object). *Let $D \in \mathbb{R}^+$, and let $f \in Lip_C(\alpha, \mathbb{R}^2)$ such that $f(x, y) = 0$ whenever $|x| + |y| \geq D$. Then $T_N^s[D, f_N^D](x)$, where f_N^D is given by Definition 5.2, converges to $T^s[D, f](x)$ uniformly in $x \in [-D, D]$ and $s \in [-1, 1]$.*

Proof. It is sufficient to prove the theorem for $D = \pi$ since we can always scale the variables x and y . This affects the constant C in $Lip_C(\alpha, \mathbb{R}^2)$, but does not affect α . In the context of X-ray tomography, $f(x, y)$ describes a physical object, and therefore scaling x and y corresponds to a change in the metric units.

By definition, $T^s[D, f](x) = T[D, f_s](x)$. By the note from Definition 5.2, for any function $g : \mathbb{R}^2 \rightarrow \mathbb{R}$ we have $g_N^D = g_N$ when $D = \pi$. Therefore, for $D = \pi$ we have

(43)

$$|T^s[D, f](x) - T_N^s[D, f_N^D](x)| = \left| T[D, f_s](x) - \frac{2\pi}{M} \sum_{v=-N}^N f_N \left(x + s \frac{2\pi}{M} v, \frac{2\pi}{M} v \right) \right|$$

(44) $\leq \left| T[D, f_s](x) - \frac{2\pi}{M} \sum_{v=-N}^N f \left(x + s \frac{2\pi}{M} v, \frac{2\pi}{M} v \right) \right|$

(45) $+ \left| \frac{2\pi}{M} \sum_{v=-N}^N \left(f \left(x + s \frac{2\pi}{M} v, \frac{2\pi}{M} v \right) - f_N \left(x + s \frac{2\pi}{M} v, \frac{2\pi}{M} v \right) \right) \right|.$

The expression in (44) can be written as $|T[D, f_s](x) - T_N[D, f_s](x)|$. By Lemma 5.7, for any $s \in [-1, 1]$, the function f_s belongs to $Lip_{C(\sqrt{3})\alpha}(\alpha, \mathbb{R}^2)$. By Theorem 5.11, the expression in (44) tends to zero uniformly in both $x \in [-\pi, \pi]$ and $s \in [-1, 1]$ as N grows.

Next we consider (45). For a fixed $v \in [-N : N]$, we denote $g_v(x) = f(x, \frac{2\pi}{M}v)$. This function belongs to $Lip_C(\alpha, \mathbb{R})$. By Lemma 5.3 we have $g_{v_N}(x) = f_N(x, \frac{2\pi}{M}v)$. The function $g_v(x)$ satisfies $g_v(x) = 0$ for $|x| \geq \pi - \frac{2\pi}{M}v$. From Lemma 5.5 there exists a function $\Phi(C, \alpha, N)$ that tends to zero as N grows such that for any $s \in [-1, 1]$ and $x \in [-\pi, \pi]$ we have $|g_v(x + s \frac{2\pi}{M}v) - g_{v_N}(x + s \frac{2\pi}{M}v)| \leq \Phi(C, \alpha, N)$. It is important to note that the function $\Phi(C, \alpha, N)$ does not depend on v . By expanding the definition of $g_v(x)$, we see that for any $v \in [-N : N]$, $s \in [-1, 1]$, and $x \in [-\pi, \pi]$ the following inequality holds:

$$\left| f \left(x + s \frac{2\pi}{M} v, \frac{2\pi}{M} v \right) - f_N \left(x + s \frac{2\pi}{M} v, \frac{2\pi}{M} v \right) \right| \leq \Phi(C, \alpha, N).$$

For any $\varepsilon > 0$ there exists N_0 such that for any $N > N_0$ we have $|\Phi(C, \alpha, N)| < \frac{\varepsilon}{2\pi}$. Therefore, for $N > N_0$ the expression in (45) is less than ε for any $x \in [-\pi, \pi]$ and $s \in [-1, 1]$. \square

5.4. 2D discrete Radon transform approximates the continuous Radon transform. Let $D \in \mathbb{R}^+$, and let $A(D) = \{(x, y) \mid -\frac{D}{2} < x < \frac{D}{3}, -\frac{D}{2} < y < \frac{D}{3}\}$. Throughout this section we assume that the function $f(x, y)$ satisfies $f(x, y) = 0$ for $(x, y) \notin A(D)$. This assumption is imposed only for convenience, to simplify subsequent proofs. The bounds in the definition of $A(D)$ are technical assumptions that ensure that $f(\frac{2D}{M}u, \frac{2D}{M}v) = 0$ whenever $u \notin [-\frac{N}{2} : \frac{N}{2} - 1]$ or $v \notin [-\frac{N}{2} : \frac{N}{2} - 1]$.

THEOREM 5.15. Let $D \in \mathbb{R}^+$. Let $f : \mathbb{R}^2 \rightarrow \mathbb{R}$ be a function such that $f(x, y) = 0$ whenever $(x, y) \notin A(D)$. Consider the array

$$(46) \quad I(u, v) = f\left(\frac{2D}{M}u, \frac{2D}{M}v\right), \quad u, v \in \left[-\frac{N}{2} : \frac{N}{2} - 1\right].$$

Then, for any $w \in [-N : N]$ and $s \in [-1, 1]$ we have

$$T_N^s[D, f_N^D]\left(\frac{2D}{M}w\right) = \frac{2D}{M} \text{Radon}(\{x = w + sy\}, I),$$

where $\text{Radon}(\{x = w + sy\}, I)$ is given in Definition 2.1.

The proof easily follows from Definitions 5.2 and 2.1, (46), and the fact that $f(x, y) = 0$ whenever $(x, y) \notin A(D)$.

When the function $f(x, y)$ represents an object that is bounded in space, it is always possible to find such a D that the conditions of Theorem 5.15 are satisfied. If, in addition, we assume that $f \in \text{Lip}_C(\alpha, \mathbb{R}^2)$ for some C and α , then we can use the 2D discrete Radon transform to approximate the continuous Radon transform of this object. We prove it formally in Theorem 5.16.

THEOREM 5.16. Let $D \in \mathbb{R}^+$, $C \in \mathbb{R}^+$, and $\alpha \in (0, 1]$. Let $f \in \text{Lip}_C(\alpha, \mathbb{R}^2)$ such that $f(x, y) = 0$ whenever $(x, y) \notin A(D)$. For an arbitrary $N \in \mathbb{N}$ we define the array I_N by

$$(47) \quad I_N(u, v) \triangleq f\left(\frac{2D}{M}u, \frac{2D}{M}v\right), \quad u, v \in \left[-\frac{N}{2} : \frac{N}{2} - 1\right].$$

Then, for any $\varepsilon > 0$ there exists $N_0 \in \mathbb{N}$ such that for any $N > N_0$

$$\left| \mathfrak{R}_y f\left(s, \frac{2D}{M}w\right) - \sqrt{1 + s^2} \frac{2D}{M} \text{Radon}(\{x = w + sy\}, I_N) \right| < \varepsilon$$

for any $w \in [-N : N]$ and any $s \in [-1, 1]$.

Proof. Fix $\varepsilon > 0$ and let $s \in [-1, 1]$. Under the conditions imposed on f in the statement of the theorem, $\mathfrak{R}_y f(s, t)$ is given by (38) when $t \in [-D, D]$ and equals zero outside this interval. Using Definition 5.12, we rewrite (38) as

$$(48) \quad \mathfrak{R}_y f(s, t) = \sqrt{1 + s^2} T^s[D, f](t), \quad t \in [-D, D].$$

By Theorem 5.14, there exists N_0 such that for any $N > N_0$

$$|T^s[D, f](x) - T_N^s[D, f_N^D](x)| < \frac{\varepsilon}{\sqrt{2}}$$

for any $x \in [-D, D]$ and $s \in [-1, 1]$. Then,

$$\left| \sqrt{1 + s^2} T^s[D, f]\left(\frac{2D}{M}w\right) - \sqrt{1 + s^2} T_N^s[D, f_N^D]\left(\frac{2D}{M}w\right) \right| < \varepsilon$$

for any $w \in [-N : N]$ and $s \in [-1, 1]$. Replacing the first term in this inequality by $\mathfrak{R}_y f\left(s, \frac{2D}{M}w\right)$ (see (48)) and applying Theorem 5.15, we get the required result. \square

Theorem 5.16 states that the continuous Radon transform of an object for lines with intercepts $\{\frac{2D}{M}w \mid w \in [-N : N]\}$ can be approximated by means of the discrete Radon transform applied to a Cartesian set of samples of this object.

Theorem 5.16 was formulated and proved for $\mathfrak{R}_y f(s, t)$, which corresponds to projections along basically vertical lines. An analogous theorem can be proved for $\mathfrak{R}_x f(s, t)$ and basically horizontal lines by minor modifications of the proofs in sections 5.3–5.4.

6. Relation to earlier work. The key structural feature of our notion of Radon transform is to parametrize by slope and to sample equispaced in slope. This idea has been used in geophysics for a long time, as a concept for digital implementation, at least since the late 1960s, where the name “Slant Stack” is commonly applied [8]. Stacking is the process of projecting a 2D array down to a 1D array by summing along one of the two coordinates. Slanting is the process of shearing the array before such stacking. Lemma 3.8 above shows that our definition has exactly such a slant stack interpretation. An earlier version of this paper used the slant stack terminology [2] and explained this connection through figures and examples. Note that the present paper improves on [2] in the use of $m = 2n + 1$ ([2] used $m = 2n$), which preserves the real-valuedness of projections of real-valued images.

In medical tomography, the continuous Radon transform is typically discussed using the traditional angle-intercept coordinates that we have used in the introduction. However, Edholm and Herman [10] introduced the notion of collecting tomographic data with projections equispaced in slope rather than angle and found fast algorithms for reconstruction from such data. Our proposal differs from their original proposal in the use of $m = 2n + 1$ rather than $m = n$, although the implementation paper with Roberts [11] did in fact use $m = 2n + 1$ for reconstruction. The main divergence between our approach and that of [10] is therefore in our attempt to define both forward and inverse Radon transforms for the digital setting, and to preserve certain exactness properties; such issues do not arise in medical tomography, where the data are gathered by a physical device and only approximate reconstruction is an issue.

7. Further properties for the discrete Radon transform defined here.

Inverting the Radon transform in the continuous case is ill-posed, and that continues to be the case for our transform. However, just as in the continuous transform case, there is a natural way to understand this ill-posedness by Fourier analysis. Recall [8] that inverting the continuous Radon transform can be accomplished by using the projection-slice theorem to transform into Fourier space, followed by multiplication with r followed by inverse Fourier transform. Symbolically, this means

$$\mathfrak{R}^* \mathfrak{R} = \mathcal{F}^* \circ (1/r^2) \circ \mathcal{F},$$

with \mathfrak{R} and \mathcal{F} being the continuous Radon and Fourier transforms, respectively, and $1/r^2$ denotes the operator of multiplication by $1/r^2$. In the companion paper [1] we exhibit an explicit preconditioner for inverting the pseudopolar Fourier transform (ppFT). Roughly speaking, the meaning of this preconditioner is the following: we can almost invert the discrete Radon transform by applying the projection-slice theorem to pass to the pseudopolar Fourier domain, then we apply an explicit r -style weight, and then we apply the adjoint ppFT. In a certain sense

$$R^* R \approx \mathcal{F}_{pp}^* \circ (1/r^2) \circ \mathcal{F}_{pp}.$$

We define in that paper a certain diagonal matrix M so that

$$\|R^* M R - Id\| < c < 1.$$

In this display the norm is the operator norm. This diagonal matrix is constant along the pseudoangle variable in the pseudopolar grid, and it scales with pseudoradius ρ like $1/\rho^2$. For an $m = 2n$ version of the definition, the earlier paper [2] showed that $c < .2$. It follows that, very nearly, our 2D Radon transform is diagonalized by ppFT. In fact, for each θ there is a simple convolution operator Υ that one can apply to

constant θ slices of the discrete Radon transform such that $\tilde{R} = \Upsilon \circ R$ is almost an isometric image of I : $\|\tilde{R}^* \tilde{R} - Id\| < c < 1$. This point of view was developed in [2].

These near-isometry properties are very valuable for applications; they allow us to build overcomplete systems of representation which are naturally associated to integrals along lines. Digital ridgelets and curvelets have been built this way [9, 7].

Finally, we remark that the intimate connection with shearing (Lemma 3.8) has numerous implications for this transform which remain to be fully exploited.

8. Conclusions. We developed a 2D discrete Radon transform, derived its main properties, and presented fast algorithms for its computation and inversion. The discrete transform is based on a rigorous definition, where each step in the construction is chosen to achieve some desirable property. As a result, the transform does not use inexact interpolation schemes, preserves the concept of summation along straight lines, and is rapidly computable and invertible.

We proved a projection-slice theorem that relates the discrete Radon transform to the pseudopolar Fourier transform of the underlying image. The fast algorithms for the pseudopolar Fourier transform provide fast forward and inverse algorithms for the discrete Radon transform.

Finally, we proved that the discrete Radon transform converges to the continuous Radon transform. This enables the discrete Radon transform to be used as an approximation to the continuous Radon transform in digital implementations.

REFERENCES

- [1] A. AVERBUCH, R. R. COIFMAN, D. L. DONOHO, M. ISRAELI, AND Y. SHKOLNISKY, *A framework for discrete integral transformations I—The pseudopolar Fourier transform*, SIAM J. Sci. Comput., 30 (2008), pp. 764–784.
- [2] A. AVERBUCH, R. R. COIFMAN, D. L. DONOHO, M. ISRAELI, J. WALDÈN, AND Y. SHKOLNISKY, *Fast Slant Stack: A Notion of Radon Transform for Data in a Cartesian Grid Which Is Rapidly Computible, Algebraically Exact, Geometrically Faithful and Invertible*, manuscript, 2001.
- [3] G. BEYLKIN, *Discrete Radon transform*, IEEE Trans. Acoustics, Speech, Signal Process., 35 (1987), pp. 162–172.
- [4] M. L. BRADY, *A fast discrete approximation algorithm for the Radon transform*, SIAM J. Comput., 27 (1998), pp. 107–119.
- [5] A. BRANDT AND J. DYM, *Fast calculation of multiple line integrals*, SIAM J. Sci. Comput., 20 (1999), pp. 1417–1429.
- [6] A. BRANDT, J. MANN, M. BRODSKI, AND M. GALUN, *A fast and accurate multilevel inversion of the Radon transform*, SIAM J. Appl. Math., 60 (1999), pp. 437–462.
- [7] E. CANDÈS, L. DEMANET, D. DONOHO, AND L. YING, *Fast discrete curvelet transforms*, Multiscale Model. Simul., 5 (2006), pp. 861–899.
- [8] S. R. DEANS, *The Radon Transform and Some of Its Applications*, revised ed., Krieger Publishing Company, Melbourne, FL, 1993.
- [9] D. L. DONOHO AND A. G. FLESIA, *Digital ridgelet transform based on true ridge functions*, in *Beyond Wavelets*, vol. 10, J. Stoecker and G. V. Welland, eds., Academic Press, New York, 2003, pp. 1–30.
- [10] P. EDHOLM AND G. T. HERMAN, *Linograms in image reconstruction from projections*, IEEE Trans. Medical Imaging, 6 (1987), pp. 301–307.
- [11] P. EDHOLM, G. T. HERMAN, AND D. A. ROBERTS, *Image reconstruction from linograms: Implementation and evaluation*, IEEE Trans. Medical Imaging, 7 (1988), pp. 239–246.
- [12] K. FOURMONT, *Schnelle Fourier-transformation bei nichtäquidistanten Gittern und tomographische anwendungen*, Ph.D. thesis, Universität Münster, Münster, Germany, 1999.
- [13] W. A. GÖTZ AND H. J. DRUCKMÜLLER, *A fast digital Radon transform—An efficient means for evaluating the Hough transform*, Pattern Recognition, 28 (1995), pp. 1985–1992.
- [14] T. C. HSUNG, D. P. K. LUN, AND W. C. SIU, *The discrete periodic Radon transform*, IEEE Trans. Signal Process., 44 (1996), pp. 2651–2657.
- [15] A. K. JAIN, *Fundamentals of Digital Image Processing*, Prentice–Hall, Englewood Cliffs, NJ, 1989.

- [16] B. T. KELLEY AND V. K. MADISETTI, *The fast discrete Radon transform. I. Theory*, IEEE Trans. Image Process., 2 (1993), pp. 382–400.
- [17] F. MATUS AND J. FLUSSER, *Image representation via a finite Radon transform*, IEEE Trans. Pattern Anal. Machine Intell., 15 (1993), pp. 996–1006.
- [18] I. SEDELNIKOV, *Discrete Diffraction Transform*, Master's thesis, School of Computer Science, Tel-Aviv University, Tel-Aviv, Israel, 2004.
- [19] A. ZYGMUND, *Trigonometric Series*, 2nd ed., Cambridge University Press, Cambridge, UK, 1993.